Malaysian Journal of Analytical Sciences (MJAS)



Published by Malaysian Analytical Sciences Society

Fe₃O₄-DOPED POLYSULFONE MEMBRANE FOR ENHANCED ADSORPTION OF COPPER FROM AQUEOUS SOLUTION

(Membran Polisulfon Berdop Fe₃O₄ untuk Peningkatan Penjerapan Kuprum daripada Larutan Akues)

Wan Khairunnisa Wan Ramli^{1*}, Nur Maisyatul Syalina Abdul Wahab¹, Siti Khalijah Mahmad Rozi^{1,2}, Syumayyah Rasis¹, Gavin Chew Tiong Chuen¹, and Lew Guo Liang¹

¹Faculty of Chemical Engineering and Technology, Universiti Malaysia Perlis, Kompleks Pusat Pengajian Jejawi 3, 02600 Arau, Perlis, Malaysia

²Centre of Excellence for Biomass Utilization, Universiti Malaysia Perlis, 02600 Arau, Perlis, Malaysia

*Corresponding author: wankhairunnisa@unimap.edu.my

Received: 3 November 2023; Accepted: 12 February 2024; Published: 29 April 2024

Abstract

Water pollution, especially from industrial wastewater has become one of the major global environmental problems. As the result of rapid industrialization, the expansion of industries such as the electroplating industry has resulted in an increase in heavy metals effluent, especially copper, in the wastewater, and this poses detrimental effects on the biodiversity and environment. The abatement of copper pollution has received widespread attention, and continuous research advancement has been observed in adsorption and membrane technology. Nanofiltration membranes with nanopores recorded higher suitability to remove ions but at the expense of membrane fouling as a result of the formation of contaminants on the surface layer that blocks the diffusion of contaminants into the membrane substructure. This research highlights the incorporation of Fe₃O₄ nanoparticles into the polysulfone (PSf) membrane matrix as an adsorptive membrane and their possible adsorption mechanism towards Cu, which can manifest the combined characteristics of both removal techniques. Fe₃O₄ nanoparticles were synthesized using the co-precipitation method. Fe₃O₄-doped PSf membranes were then synthesized with various concentrations of Fe via the Non-solvent Induced Phase Separation (NIPS) technique. The physicochemical properties of the Fe nanoparticles and the membranes were evaluated using Xray diffraction (XRD), Scanning Electron Microscope (SEM), water contact angle and porosity testing. Crystal phase analysis confirmed the formation of magnetite Fe₃O₄ in a cubic structure. Agglomerations of Fe NPs on the membrane surface were observed for membranes with lower Fe concentrations, suggesting the possibility of poor blending and this contributed to the lower adsorption capability of these membranes. Membranes with 2 wt.% Fe concentration (Fe-2.0) exhibited the highest Cu(II) ions adsorption capacity of 637 mg/g, which is trifold of those recorded for pristine PSF membrane (Fe-0.0). The adsorption data of Cu adsorption were best fitted into the Temkin isotherm and pseudo-second-order models, suggesting an adsorption mechanism involving an exothermic chemical interaction between Cu ions and the Fe₃O₄ NPs within the membrane. This research confirms the potential of incorporating Fe₃O₄ in the PSf membrane backbone to enhance Cu removal as an adsorptive membrane, even at lower NP concentrations.

Keywords: adsorptive membrane, copper removal, iron oxide, adsorption kinetics

Wan Ramli et al.: Fe₃O₄-DOPED POLYSULFONE MEMBRANE FOR ENHANCED ADSORPTION OF COPPER FROM AQUEOUS SOLUTION

Abstrak

Pencemaran air, terutamanya daripada air sisa industri telah menjadi salah satu masalah alam sekitar yang utama di seluruh dunia. Berikutan pengindustrian yang pesat, peluasan industri seperti industri penyaduran elektrik telah mengakibatkan peningkatan dalam efluen logam berat, terutamanya kuprum, dalam air buangan, dan ini menimbulkan kesan buruk kepada biodiversiti dan alam sekitar. Pengurangan pencemaran kuprum telah mendapat perhatian yang meluas, dan kemajuan penyelidikan berterusan telah diperhatikan dalam teknologi penjerapan dan membran. Membran penapisan nano dengan liang bersaiz nano mencatatkan kesesuaian yang lebih tinggi untuk menyingkirkan ion tetapi dengan mengorbankan penyisikan membran akibat pembentukan lapisan permukaan bahan cemar yang menghalang resapan bahan cemar ke dalam substruktur membran. Penyelidikan ini menekankan penggabungan nanopartikel Fe₃O₄ ke dalam matriks membran polisulfon (PSf) sebagai membran penjerap dan mekanisme penjerapan yang mungkin terhadap Cu, yang boleh menunjukkan ciri gabungan kedua-dua teknik penyingkiran tersebut. Nanozarah Fe₃O₄ disintesis menggunakan kaedah pemendakan bersama. Membran PSf terdop Fe kemudiannya disintesis dengan pelbagai kepekatan Fe melalui teknik pemisahan fasa teraruh bukan pelarut (NIPS). Sifat fizikokimia nanopartikel Fe dan membran dinilai menggunakan pembelauan sinar-X (XRD), mikroskop elektron pengimbasan (SEM), sudut sentuhan air dan ujian keliangan. Analisis fasa kristal mengesahkan pembentukan magnetit Fe₃O₄ dalam struktur kubus. Aglomerasi NP Fe pada permukaan membran diperhatikan untuk membran dengan kepekatan Fe yang lebih rendah, menunjukkan kemungkinan pengadunan yang lemah dan ini menyumbang kepada keupayaan penjerapan yang lebih rendah bagi membran ini. Membran dengan kepekatan Fe 2% berat (Fe-2.0) mempamerkan kapasiti penjerapan ion Cu(II) tertinggi sebanyak 637 mg/g, iaitu tiga kali ganda daripada yang direkodkan untuk membran PSF murni (Fe-0.0). Data penjerapan penjerapan Cu paling baik dipadankan ke dalam model isoterma Temkin dan pseudo-second-order, mencadangkan mekanisme penjerapan yang melibatkan interaksi kimia eksotermik antara ion Cu dan NP Fe₃O₄ dalam membran. Penyelidikan ini mengesahkan potensi menggabungkan Fe₃O₄ dalam tulang belakang membran PSf untuk meningkatkan penyingkiran Cu sebagai membran penjerap, walaupun pada kepekatan NP yang lebih rendah.

Kata kunci: membran penjerap, penyingkiran kuprum, ferum oksida, isoterma penjerapan, kinetik penjerapan

Introduction

The rapid growth of urban industrialization, including the chemical industries, uses enormous amounts of water and produces large amounts of waste effluent during the production processes. Copper (Cu), chromium (Cr), zinc (Zn), and cadmium (Cd) are the most common heavy metals present in these industrial effluents, making the release of heavy metals from such operations far more dangerous [1]. In fact, the electroplating industry alone produces a high amount of copper, in the range of 8.8 g/L [2]. These heavy metals are stable, non-biodegradable, toxic, and carcinogenic. They accumulate in living organisms and can cause severe problems for public health and the environment. The Environmental Protection Agency (EPA) has set the acceptable standard concentrations of Cu that can be discharged from industries to the environment, which falls within the range of 0.2 and 1.0 mg/L. Therefore, the remediation of water contaminated by Cu is critical to protect the environment as well as to promote water reuse.

Increased interest was observed towards membrane filtration, mainly ultrafiltration (UF) and nanofiltration

(NF). UF is replacing the conventional method for water treatment and is becoming universally accepted due to the lower operating pressure and the simple membrane preparation, among others. However, small compounds and toxic ions cannot be removed using UF. Meanwhile, nanofiltration (NF) is used to remove heavy metals from water, but the performance of the NF membrane, is restricted by the species of the targeted heavy metal and the fact that it degrades as heavy metal concentrations increase up to 2000 mg/L [3]. In addition, NF membranes require higher mechanical strength, owing to the higher operating pressure and the functional surface layer that is critical to ensure the efficacy of the membrane separation. These often require complicated preparation of the functional surface layer such as interfacial polymerization and surface coating [4]. Polysulfone (PSf) membrane is often used in NF membrane formation due to its high chemical and mechanical resistance, but its hydrophobic nature often results in low flux and membrane fouling [5]. This has triggered the rapid development of efficient and costeffective membranes for heavy metal removal, particularly Cu, which can overcome the limitations of NF and other common remediation techniques. The

invention of adsorptive membranes that combine the advantages of both adsorption and membrane filtration can also overcome the drawbacks of both techniques. The impregnation of prospective nano adsorbents into polymeric membranes can be achieved by characterizing them based on their affinity towards pollutants in the forms of ions and molecules [6].

Hydrophilic nanoparticles are often used to boost the hydrophilicity and flux of the PSf membrane, especially in removing Cu. The findings of Ayaz et al. [7] indicated that adding hydrophilic nanoparticles such as alumina into the PSf membrane matrix can increase the hydrophilicity of the membrane. This subsequently increases the water flux and Cu rejection from 40% for the nascent PSf membrane to 75% for PSf membrane with 1 wt.% alumina. Zeolite is also used in the PSf membrane to remove Cu. Hamid et al. [8] reported that the highest Cu adsorption capacity of 101 mg/g for PSf membrane doped with 15 wt.% of zeolite at an optimum pH of 5 as well as the anionic character of zeolite, attract the positive Cu ions for the adsorption process. Iron oxide nanoparticles have been amalgamated into membrane matrix due to their strong affinity towards Cu and hydrophilic nature, which can increase the hydrophilicity of PSf membranes in order to enhance the membrane performance towards not only Cu but other heavy metals. This includes lead [9], phosphate [10] and other contaminants such as protein. Said et al. [11] reported increased water flux and protein rejection with the addition of iron oxide into their PSf membrane, attributed to the higher porosity and hydrophilicity. Even though iron oxide has been reported as a popular nano adsorbent in many reports involving polymeric adsorptive membranes to remove heavy metals, the adsorption mechanism towards Cu (II) ions in highly concentrated copper aqueous solution has never been reported previously.

In this present work, the adsorption capability and mechanism of the Fe₃O₄-doped PSf membrane were evaluated. A set of adsorptive membranes was synthesized by incorporating various concentrations of Fe₃O₄ NPs into the PSf membrane matrix to remove Cu from the aqueous solution. The Fe₃O₄ NPs were prepared via the common co-precipitation method and

the membranes were synthesized via the simple nonsolvent induced phase separation (NIPS) technique. The Fe_3O_4 NPs were characterized using XRD and the membranes were evaluated using FTIR, SEM, contact angle measurement and porosity analysis. The adsorption performance of the membranes was evaluated in terms of contact time and initial Cu concentrations. Subsequently, the adsorption mechanism of these membranes was also evaluated.

Materials and methods

Chemicals

Metal precursors such as FeCl₂.6H₂O, (NH₄)₂ Fe(SO₄)₂.6H₂O and CuSO₄ powders were procured from R&M chemicals. Polysulfone (PSf) polymer pellets were procured from Solvay Solexis (France). Dimethylacetamide (DMAc, 99.5%), used as the solvent, was purchased from Sigma-Aldrich (Germany). Ultrapure deionized water was used as the coagulant. All solvents and precursors were used as received.

Instrumentation

X-ray diffraction (XRD) pattern of the synthesized Fe nanoparticles was recorded using a diffractometer (Bruker AXS Inc., 30 kV, 10 mA), and equipped with a Cu-K α radiation source ($\lambda = 1.5412$ Å). The samples were scanned from 15° to 70° (20). Surface morphological analysis of Fe₃O₄-doped PSf membranes was carried out using Hitachi SU8220 Scanning Electron Microscopy (Oxford Instrument, Oxford Shire, UK). FTIR spectra were recorded on Perkin Elmer FTIR spectrophotometer (Massachusetts, USA) with a crystal diamond universal ATR sampling accessory at room temperature. All spectra were recorded in the wavenumber range of 4000 to 500 cm⁻¹. The membrane porosity was measured using the gravimetric method. The membrane was immersed in ethanol for 2 hours. The wet membrane was then slightly patted to remove excess liquid on the surface and weighed to get the weight of the wet membrane, w_m. The membrane was then dried in an oven for an additional 2 hours and the weight of the dried membrane, w_d was weighed. The membrane porosity can be calculated using Equation 1:

$$\varepsilon = \frac{(w_m - w_d)/\rho_e}{((w_m - w_d)/\rho_e) + (w_d/\rho_p)} \tag{1}$$

where w_m is the weight of the wet membrane (g), w_d is the weight of the dry membrane (g), ρ_e is the density of ethanol and ρ_p is the density of the polymer, PSf. The water contact angle of the membrane surface was evaluated using the sessile drop method. A water droplet of 2 μ L was dropped on the membrane surface and images of the droplet were taken after 5 s. The images were analysed using the ImageJ software to get the water contact angle of the membrane [12,13].

Synthesis of Fe₃O₄ nanoparticles

The Fe₃O₄ nanoparticles were synthesized via the coprecipitation method. High-purity precursors including FeCl₂.6H₂O (3.9 g) and Fe(SO₄)₂.6H₂O (5.4 g) were used in appropriate stoichiometric molar ratios. The precursors were dissolved in 200 mL of deionized water under vigorous stirring until a suspension solution was formed. A concentrated NaOH solution was then added dropwise until the pH of the suspension achieved 7 (Neutral). The suspension was vigorously stirred for 2 h before repeatedly washing with deionized water to remove the excess NaOH. The formed suspension was then filtered and dried in the oven at 110 °C for 5 h. The dried nanoparticle powders were kept in a desiccator prior to characterization and testing [3,14].

Synthesis of Fe₃O₄-doped PSf membranes

The Fe₃O₄-doped PSf membranes were prepared following the formulation shown in Table 1, via the phase separation method, particularly the Nonsolvent Induced Phase Separation (NIPS) method (Figure 1). Dope solutions with various wt.% of nanoparticles were prepared. DMAc was first heated to 60 °C, with constant stirring and pre-weighed PVP at 1 wt.% was added to the solvent as a pore former. Next, various wt.% of nanoparticles prepared in the previous subsection were added slowly to the solution [15]. Dried PSf granules at 18 wt.% were then gradually added and dissolved into the solution for 6 h. After mixing, the dope solution was degassed prior to casting, to remove any bubbles formed during the stirring process. The dope solution was then cast onto a glass plate using a casting machine, with a membrane thickness of 250 µm. The casted solution was then immediately immersed into a coagulation bath, containing deionized water for the phase inversion process to occur. The membrane formed was then washed to remove any excess solvent and dried at ambient temperature. The membrane was then placed in fresh DI water prior to characterization and performance tests.

Table 1. Composition of the synthesized Fe₃O₄-doped PSf membranes

1	,			
Membrane	PSf,	PVP,	DMAc,	Fe NPs,
	(wt.%)	(wt.%)	(wt.%)	(wt.%)
Fe-0.0	18	1	81.0	0.0
Fe-0.5	18	1	80.5	0.5
Fe-1.0	18	1	80.0	1.0
Fe-2.0	18	1	79.0	2.0

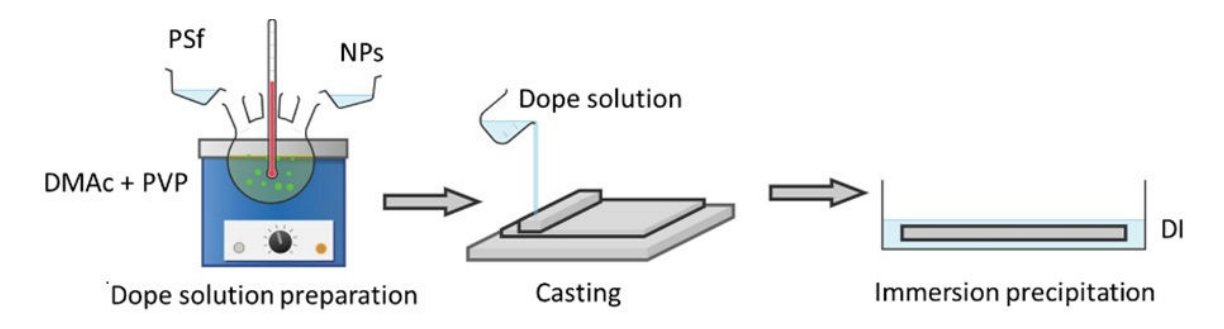


Figure 1. Fe₃O₄-doped PSf membrane preparation via NIPS

Batch adsorption studies

The batch adsorption study was performed to evaluate the adsorption characteristics of Fe₃O₄-doped PSf membranes towards copper. Effects of contact time and initial concentration on the adsorption capacity, q and copper rejection, R of the synthesized membranes were evaluated using Equation 2 and 3.

$$q_e = \frac{(C_o - C_e)V}{m} \tag{2}$$

$$q_e = \frac{(c_o - c_e)V}{m}$$

$$R = \left[1 - \left(\frac{c_e}{c_o}\right)\right] \times 100\%$$
(2)

where q is the adsorption capacity (mg/g), Co and Ce are the initial and equilibrium concentration of metal ions in solution (mg/L), V is the volume of the solution (L) and m is the membrane dry mass (g).

The adsorption experiments were performed in batches and the effects of Cu initial concentration and contact time on Cu removal were evaluated. 12.5 mg of the membranes with various wt.% of Fe nanoparticles were cut into smaller pieces and placed into several centrifuge tubes containing 12.5 mL of various initial concentrations of Cu solution; from 0.05 to 1.2 M. The tubes were agitated at 160 rpm for 30 minutes. To study the effect of contact time, the membranes were placed into 0.05 M of Cu solution and were removed from the solution after 5, 10, 15, 20, 25 and 30 minutes, respectively. The final concentration of the Cu solution was measured using a UV-Vis spectrophotometer.

Adsorption Isotherm and Kinetic

The mechanism of Cu adsorption onto the Fe₃O₄-doped PSf membranes was further evaluated based on three isotherms models;1. Langmuir, 2. Freundlich and 3. Temkin. These isotherm models are best described based on the following linear equations as shown in Equations 4 to 6, respectively:

$$\frac{c_e}{q_e} = \frac{1}{q_{max}K_L} + \frac{c_e}{q_{max}}$$

$$ln q_e = \ln K_f + \frac{1}{n} ln C_e$$

$$q_e = \frac{RT}{b_T} ln K_T + \frac{RT}{b_T} ln C_e$$
(4)
(5)

$$lnq_e = \ln K_f + \frac{1}{n} lnC_e \tag{5}$$

$$q_e = \frac{RT}{h_T} lnK_T + \frac{RT}{h_T} lnC_e \tag{6}$$

where qe is the equilibrium adsorption capacity (mg/g), q_{max} is the maximum adsorption capacity (mg/g), C_e is the equilibrium concentration of metal ions (mg/L) and K_L is the Langmuir adsorption constant (L/mg), n is the adsorption intensity constant, K_f is the Freundlich adsorption constant (L/g), R is the gas constant (8.314 J/mol), T is the absolute temperature (K), K_T is the Temkin equilibrium constant (L/g) and b_T (J/mol) is the constant associated with the adsorption heat. For the Langmuir model, an important parameter, known as the separation factor or equilibrium parameter, denoted as R_L, shown in Equation 7, is used to check the favourability of Cu adsorption onto the Fe₃O₄-doped PSf membranes.

$$R_L = \frac{1}{1 + K_L C_0} \tag{7}$$

where K_L and C_o are the Langmuir constant and the highest initial concentration of Cu, respectively.

The kinetics of the adsorption were also evaluated based on these two common kinetic models; the pseudo-firstorder and pseudo-second-order models. The pseudofirst-order and pseudo-second-order models described in linear forms as Equation 8 and 9, respectively:

$$log (q_e - q_t) = log q_e - K_1 t \tag{8}$$

$$log (q_e - q_t) = log q_e - K_1 t$$

$$\frac{t}{q_t} = \frac{1}{K_2 \cdot q_e^2} + \frac{t}{q_e}$$
(8)

where K₁ (1/min) is defined as the pseudo-first-order adsorption rate constant, qe (mg/g) and qt (mg/g) are the adsorption capacities for Cu adsorption at equilibrium and at respective contact time and K₂ (g/mg min) is the pseudo-second-order rate constant.

Results and Discussion

Characterizations

The XRD pattern of the synthesized nanoparticles, shown in Figure 2 shows well-defined Bragg reflection characteristics of Fe₃O₄. The data shows diffraction peaks at $2\theta = 30.2306^{\circ}$, 35.59° , 43.4167° , 57.3511° and 56.998° which can be indexed to the (220), (311), (400), (422) and (511) planes of Fe₃O₄ in a cubic phase, respectively which is consistent with the standard pattern for magnetite Fe₃O₄ (JCPDS no.- 96–900-7645) [16]. Based on the XRD pattern, the highest peak is approximately 35.59°, indicating that the (311) plane is the most ordered plane in the crystal lattice. The crystallite size was around 15 nm to 42 nm which agrees

Wan Ramli et al.: Fe₃O₄-DOPED POLYSULFONE MEMBRANE FOR ENHANCED ADSORPTION OF COPPER FROM AQUEOUS SOLUTION

with the findings by Upadhyay et al. [17], which reported a crystallite size ranging from 27 nm to 53 nm for Fe₃O₄ nanoparticles.

Figure 3a displays the FTIR spectra of the synthesized membranes. All membranes showed similar peaks at 1585 cm⁻¹, 1488 cm⁻¹, 1242 cm⁻¹ and 1150 cm⁻¹ [18]. These peaks confirm the presence of PSf as the backbone of these membranes although the reduced intensity of the absorption peaks for Fe₃O₄-doped PSf membranes suggested that the weight percentage of PSf was affected by the addition of Fe into the membrane matrix [19]. The presence of the carbonyl and sulfone

group within the PSf polymer was confirmed by the characteristic peaks observed at approximately 558 cm⁻¹, 1242 cm⁻¹, 1150 cm⁻¹ and 1585 cm⁻¹ which correspond to the asymmetric stretching, symmetric stretching, and bending vibrations of the sulfone group, including the C-O-C, O=S=O and C=C aromatic, respectively [20, 21]. Peaks for the C-S stretching vibrations were also observed at 635 cm⁻¹ for all membrane [22]. After the addition of Fe₃O₄ NPs, the intensity of the C-S peak increases (Figure 3b), due to the presence of Fe-O bond at around 635 cm⁻¹, confirming the successful incorporation of the Fe₃O₄ nanoparticles on the PSf membrane [23].

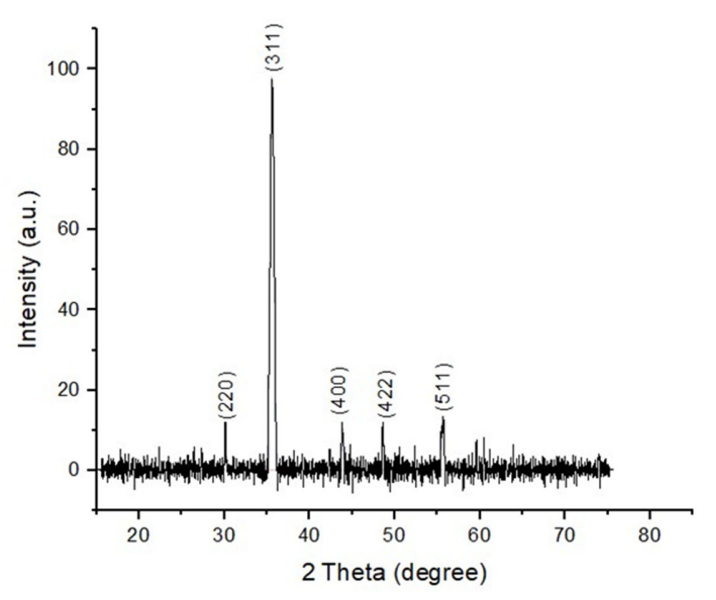


Figure 2. XRD pattern of the synthesized Fe nanoparticles

The surface morphology of Fe₃O₄-doped PSf membranes was appraised under SEM (Figure 4). Figure 4a indicates some pores on the surface of the Fe-0.0 membrane, with other visible pores, hidden under a very thin skin layer and uniformly distributed across the surface. As the concentration of Fe nanoparticles increased from 0.5 wt.% to 1.0 wt.% (Figure 4b and c), the dense skin layer thickens, evidenced by the less visible pores on the surface but at the expense of increasing Fe agglomeration on the surface layer. The blending of 2 wt.% of Fe into the PSf membrane (Figure 4d) also induced some nonsolvent penetration through the thick dense layer, forming pores on the surface and

with less Fe agglomeration. These top surface morphologies also revealed that the blending of Fe nanoparticles in the membrane matrix was improved with increasing concentration of Fe. The top surfaces of the Fe-0.5 and Fe-1.0 membranes (Figure 4b and c) were covered by white particle agglomeration and this agglomeration was significantly reduced when the Fe concentration was increased to 2 wt.%. This observation can be explained by the miscibility of PSf with PVP and Fe nanoparticles. Since PVP is hydrophilic in nature and is not miscible with PSf, thermodynamically, it facilitated the penetration into the membrane during the solvent/ nonsolvent exchange. However, kinetically,

this can also increase the viscosity of the solution. Without the addition of the Fe nanoparticles (Fe-0.0), the thermodynamic effects are more dominant, resulting in a rapid demixing process, whereby the polymer precipitates very quickly, forming a very thin skin layer and presumably with a finger-like substructure [24, 25]. The addition of Fe NPs reduces the shear force of the

dope solution due to the restricted shear flow of polymer chains by the NPs thus increasing the viscosity of the dope solution. This then potentially delayed the demixing process by slowing down the exchange between the solvent and nonsolvent in the sublayer, thus delaying the solvent polymer demixing, forming a denser skin layer before the demixing occurs [10, 26].

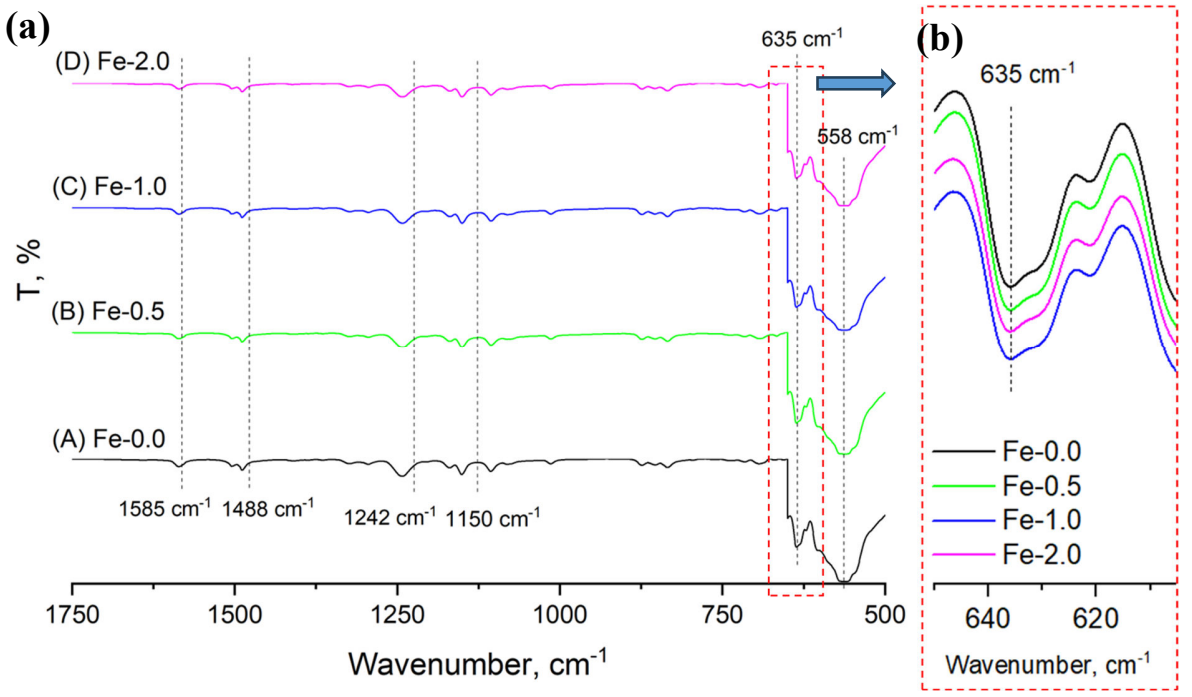


Figure 3. (a) FT-IR spectra of (A) Fe-0.0 (B) Fe-0.5, (C) Fe-1.0 and (D) Fe-2.0, and (b) FT-IR spectra of Fe-0.0, Fe-0.5, Fe-1.0 and Fe-2.0 at the Fe-O stretching band (635 cm⁻¹)

The surface hydrophobicity or the wetting capability of the membrane is considered one of the important requirements for water filtration, specifically to improve the pure water flux and prevent membrane fouling. In addition, the surface hydrophilicity of a membrane also depends on the porosity, surface roughness, and chemical composition of the surface. Lower water contact angle measurements are a sign of higher hydrophilicity, which is preferable for wastewater treatment purposes because it can draw in water molecules and prevent foulants from adhering to or interacting with the surface of the membrane, improving its antifouling abilities and water flux [27]. Figure 5 shows the water contact angle (WCA), measured using the sessile drop method and the porosity of the

membranes. As shown in Figure 5, the pristine PSf membrane exhibited a WCA of 77.40°, showing a rather hydrophobic trait against water, while other membranes revealed a decreasing trend of WCA values than that of the pristine PSf membrane (Fe-0.0) with increasing Fe concentration. Fe-0.5, Fe-1.0 and Fe-2.0 recorded WCA values of 71.96°, 53.99° and 50.93°, respectively. The hydrophilicity of the membranes improved significantly due to the hydrophilicity nature of the Fe NPs, owing to the higher surface energy and the presence of the oxygen element in the Fe NPs [28], in the form of Fe₃O₄, as corroborated by the XRD result, albeit at lower concentration of Fe NPs into the membrane matrix. This subsequently promotes chemisorption and makes it attractive as an adsorptive membrane [29].

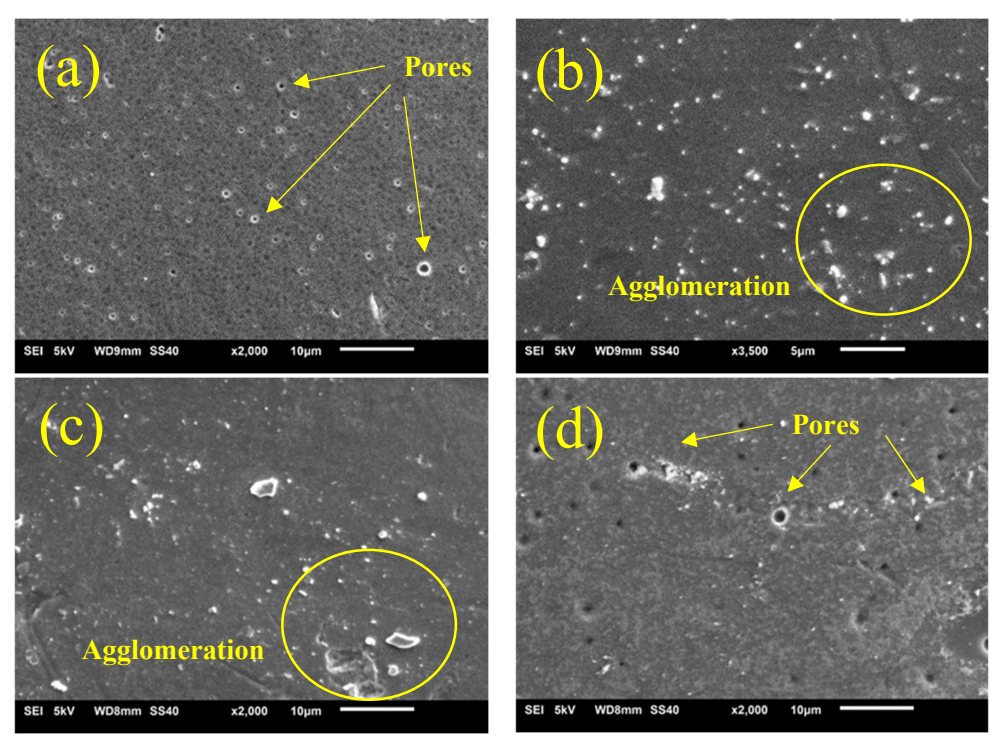


Figure 4. SEM images of the surface region of Fe₃O₄-doped PSf membranes at 2000x magnification: (a) Fe-0, (b) Fe-0.5, (c) Fe-1.0, and (d) Fe-2.0

In terms of the porosity of the membrane, a substantial decline was observed after the addition of Fe NPs, with Fe-0.5 membrane recorded the lowest porosity at 14%. This was more than half than the porosity recorded for the pristine PSf membrane (Fe-0.0) which was at 38%. Granting that the porosity of the Fe₃O₄-doped PSf membranes was lower compared to the pristine PSf membrane, the porosity immediately picks up the trend and shows a positive increase of porosity with increasing Fe concentrations. The formation of the denser skin layer at the top of the Fe-0.5, Fe-1.0 and Fe-2.0 membranes, resulting from the polymer-rich phase formation at the nonsolvent-film interface hindered the diffusion of solvent/nonsolvent of the membrane film after immersion into water. The closer porous substructure formed due to the delayed demixing subsequently increases the thickness of the top dense layer, reducing the porosity of the membrane [13]. The lower porosity of Fe-0.5 and Fe-1.0 membranes can also be attributed to the ineffective blending of Fe NPs in the membrane matrix causing the NPs to agglomerate. The

formation of larger Fe agglomerates can reduce the free space of the membrane, thus reducing the porosity [26].

Batch adsorption study fo Cu

The synthesized Fe₃O₄-doped PSf membrane was evaluated as the adsorptive membrane for Cu removal. The adsorption capacity (mg/g) and the Cu removal percentage (%) of the membranes were established under two main adsorption parameters, such as the initial Cu concentrations and the contact time. The adsorption process was evaluated with a membrane mass of 12.5 mg, and 12.5 mL of Cu solutions at 27 °C and pH 7 except otherwise stated.

Effect of Fe₃O₄ doping

Figure 6 illustrates the effect of blending Fe₃O₄ into the PSf membrane matrix on the adsorption capacity. It is evident that the adsorption capacity was improved from below 267 mg/g to almost double (514 mg/g) when only 0.5 wt.% of Fe₃O₄ was blended into the membrane. The Cu removal increases almost trifold after 30 minutes of contact with the PSf membrane with 2 wt.% of Fe (Fe-

2.0) as compared to the pristine membrane (Fe-0.0). The data revealed a clear increasing trend of adsorption capacity with increasing Fe₃O₄ concentration with the Fe-2.0 membrane recording the highest Cu adsorption capacity of 670 mg/g. The root cause of this enhancement can probably be traced back to the higher

Fe₃O₄ loading with less agglomeration, hence providing more available adsorption sites for Cu ions adsorption. Agglomerations observed for Fe-0.5 and Fe-1.0 might obstruct the potential adsorption sites for Cu ions, lowering the adsorption capacity of the membranes [3].

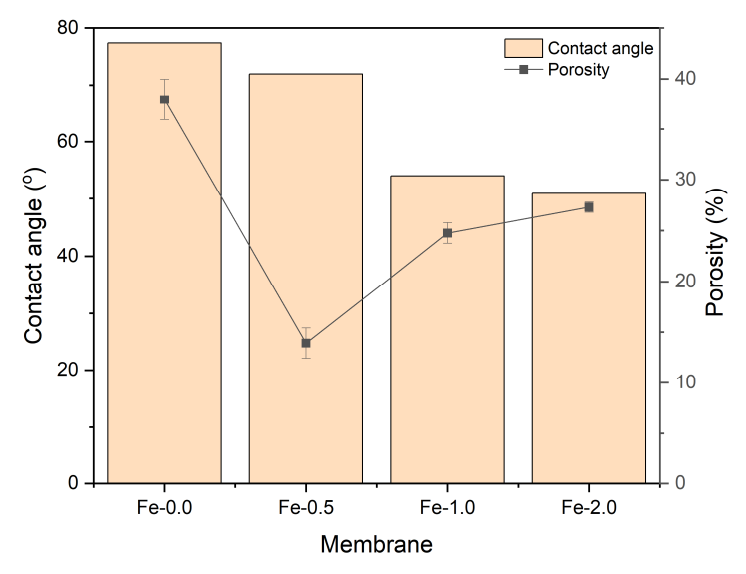


Figure 5. Water contact angle (°) and porosity of the Fe₃O₄-doped PSf membranes

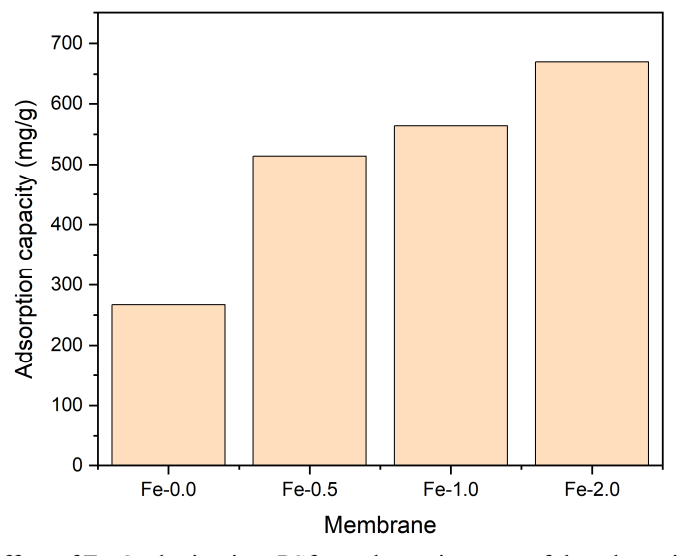


Figure 6 Effect of Fe₃O₄ doping into PSf membrane in terms of the adsorption capacity

Table 2 presents the comparison between the current work, Fe₃O₄-doped PSf membrane with previously reported adsorptive membrane for the adsorption of Cu

ion from aqueous solution in terms of the adsorption capacity. The results revealed that the proposed Fe_3O_4 -doped PSf membrane is a highly efficient adsorptive

Wan Ramli et al.: Fe₃O₄-DOPED POLYSULFONE MEMBRANE FOR ENHANCED ADSORPTION OF COPPER FROM AQUEOUS SOLUTION

membrane with the highest adsorption capacity for the treatment of Cu ions from aqueous solution. The Fe₃O₄-doped PSf membrane exhibited the highest adsorption

capacity of Cu ions with a comparable NP concentration and contact time to other reported adsorbents.

Table 2. Comparison of the synthesized adsorptive membrane with other published adsorptive membranes for adsorption of Cu ions

Membrane	Adsorbent	Concentration of Adsorbent (wt.%)	Adsorption Capacity	References
PSf	NiFe ₂ O ₄	3	42 mg/g	[30]
PES	PEG-coated	2-6	-	[31]
	CoFe ₂ O ₃			
PES	PANI/ Fe ₃ O ₄	0.01-1	1.6 mg/g	[32]
PSf	Fe_3O_4	0.5-2	670 mg/g	This work

Effect of Cu initial concentration

Figure 7 depicts the removal of Cu(II) by Fe₃O₄-doped PSf membranes at different Cu initial concentrations (0.05, 0.06, 0.07 and 0.08 M). A steady increase in Cu adsorption can be seen for all membranes with respect to increasing Cu initial concentration ranging from 0.05 to 0.08 M. This occurred as a consequence of the increasing concentration gradient, which increased the driving force for the molecules to slit into the membrane pores and adhere to the surface of the NP [15]. Additionally, a higher number of Cu ions to be adsorbed onto the NPs can also facilitate the adsorption. At a lower Cu concentration of 0.05 M, the increasing Cu

adsorption capacity was in the order of Fe-1.0 <Fe.0.5<Fe-2, while at higher Cu concentrations of 0.08 M, Fe-0.5 membrane recorded the lowest adsorption capacity of around 4613 mg/g. For membranes with lower adsorption capacity such as Fe-0.5 and Fe-1.0 membranes, the ineffective blending of the Fe NPs which results in particle agglomeration, observed in the SEM images might cause the uneven distribution of NPs in the membrane matrix subsequently reducing the number of readily available adsorption sites. These large agglomerates can also restrict the access of Cu(II) ions to the active sites on the surface of the membrane and in the membrane matrix.

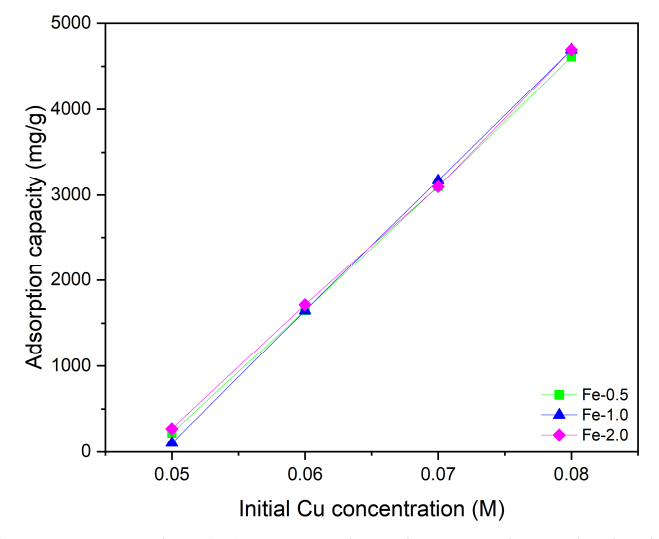


Figure 7. Effect of initial Cu concentration (M) on Cu adsorption capacity and rejection of the Fe₃O₄-doped PSf membranes (pH = 7.0 ± 0.1 , membrane dosage = 1.0 g/L, contact time = 120 min, volume of feed solution = 12.5 mL)

Effect of contact time

The effects of contact time on the adsorption capability of the synthesized Fe₃O₄-doped PSf membranes are shown in Figure 8. In general, within 30 minutes, two distinct main stages were observed in the adsorption process for all three membranes. Following the common trend of any adsorption process, the adsorption was rapid in the first 5 minutes of contact time. The adsorption capacity of the membranes increases with increased concentration of Fe in the PSf membrane with 394 mg/g, 586 mg/g and 637 mg/g for Fe-0.5, Fe-1.0 and Fe-2.0, respectively. This rapid trend was due to the bulk diffusion of Cu ions into the membrane pores followed by the sorption of the ions onto the abundant vacant Fe nanoparticles in the pores. The higher number of adsorption sites at the beginning of the adsorption

process was believed to be the driving force of this rapid Cu removal. No further increment of Cu removal was observed for the Fe-1.0 membrane as the vacant adsorption sites decreased and became saturated over time [33]. A slight difference can be observed in the adsorption process trends for Fe-0.5 and Fe-2.0 which can be attributed to the difference in morphologies of the membranes. Fe particle aggregates on the Fe-0.5 surface can also promote the adsorption of Cu on the surface particles which then blocks the penetration of more Cu into the membrane pores, slowing down the adsorption process altogether [9]. The adsorption activity of the Fe-2.0 membrane was further increased after 20 minutes, indicating that there are more available sites for Cu to adsorb hence improving the Cu removal even more.

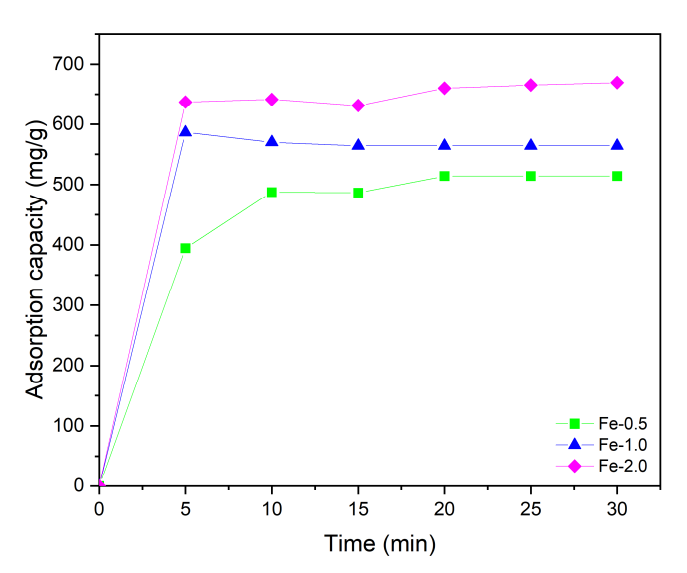


Figure 8. Effect of contact time (min) on Cu adsorption capacity and rejection of the Fe_3O_4 -doped PSf membranes (pH = 7.0±0.1, membrane dosage = 1.0 g/L, contact time = 60 min, volume of feed solution = 12.5 mL)

Evaluation of adsorption isotherm models and kinetics

In order to gain an understanding of the sorption mechanism of Cu ions onto these Fe₃O₄-doped PSf membranes, the experimental data were fitted into three main adsorption isotherms, specifically the Langmuir, Freundlich and Temkin models. The Langmuir isotherm model assumes that the adsorbate molecules are adsorbed onto a surface in a single layer, with each adsorption site having the same affinity for the

adsorbate. The model also assumes that there is no transmigration of adsorbate molecules within the plane of the surface [34]. The Freudlich isotherm model describes the adsorption of a substance onto a heterogeneous surface with active sites having different binding energies. The adsorption favours the chemical adsorption process if the value of n is <1. However, if the value of n is >1, the adsorption then adopts the physical adsorption process [35]. The Temkin isotherm model focuses on the effect of adsorbate-adsorbent

Wan Ramli et al.: Fe_3O_4 -DOPED POLYSULFONE MEMBRANE FOR ENHANCED ADSORPTION OF COPPER FROM AQUEOUS SOLUTION

interactions and the heat of adsorption on the adsorption process. It assumes a linear decrease in adsorption energy with increasing surface coverage, indicating that the adsorbate-adsorbent interactions weaken as the adsorption progresses [36].

Table 3 tabulates the isotherm parameters for all three models of all three membranes. In general, the equilibrium data of all membranes demonstrated stronger correlations with the Temkin isotherm model (Figure 9), evidenced by the higher correlation coefficients, R² of around 0.90-0.97, compared to those of the Langmuir and Freundlich isotherm models. The values obtained for the maximum adsorption capacity, q_{max} of Fe₃O₄-doped PSf membranes reveal that the adsorption of Cu onto these membranes does not follow the Langmuir isotherm. The corresponding R² for the Freundlich isotherm was higher than those of Langmuir showing a good linearity to the model. Still, the values of n did not fall within the range for favourable adsorption of between 1 to 10 [37]. Low values of n were observed for all membranes in the range of 0 to 1 indicating lower affinity between Cu ions and Fe NPs on the membrane [38], although this also suggests the adsorption involves chemisorption. The strength of the adsorption can also be described by the values of 1/n. All membranes demonstrated 1/n values above 1

indicative of cooperative adsorption whereby the adsorbed Cu ions can influence the adsorption of free Cu ions [39]. These results show that the linearized Langmuir and Freundlich models alone cannot properly describe the adsorption of Cu ions onto these membranes. As for Temkin, the variation of the adsorption energy, b_T was positive for all membranes, suggesting an exothermic sorption process between the Cu ions and the Fe_3O_4 NPs. This isotherm also validates the influence of Cu ions-Fe_3O_4 NPs interaction on the linear decrease of adsorption energy with increasing surface coverage [40].

It can also be inferred that these isotherms on their own might be underestimating the adsorption capability of these Fe₃O₄-doped PSf membranes, which contradicts the experimental data that suggests a higher performance of these membranes in removing Cu. However, the underestimation might also be due to the poor blending of the NPs resulting in huge agglomerates on the surface and in the membrane substructure. These agglomerates also occupied larger surface areas, reducing the available active sites for adsorption, hindering the proper adsorption of Cu ions onto the adsorption sites and consequently reducing the Cu removal and the misinterpretation of these isotherms [41].

Table 3. Isotherm parameters for Cu adsorption onto the Fe₃O₄-doped PSf membranes

Isotherm	Parameter	Fe-0.5	Fe-1.0	Fe-2.0
Langmuir	q _{max}	-12.3457	-8.3472	-16.1031
	b	-8119.07	-8039.9	-8077.29
	\mathbb{R}^2	0.7814	0.8540	0.7686
Freundlich	K_{f}	2.53 x 10 ⁻¹⁹	5.23 x 10 ⁻²⁴	3.43 x 10 ⁻¹⁸
	1/n	5.4230	6.5660	5.1493
	n	0.1844	0.1523	0.1942
	\mathbb{R}^2	0.8968	0.8484	0.8808
Temkin	K_{T}	0.00012	0.00015	0.00013
	b	0.0292	0.0218	0.0316
	\mathbb{R}^2	0.9722	0.9441	0.9081

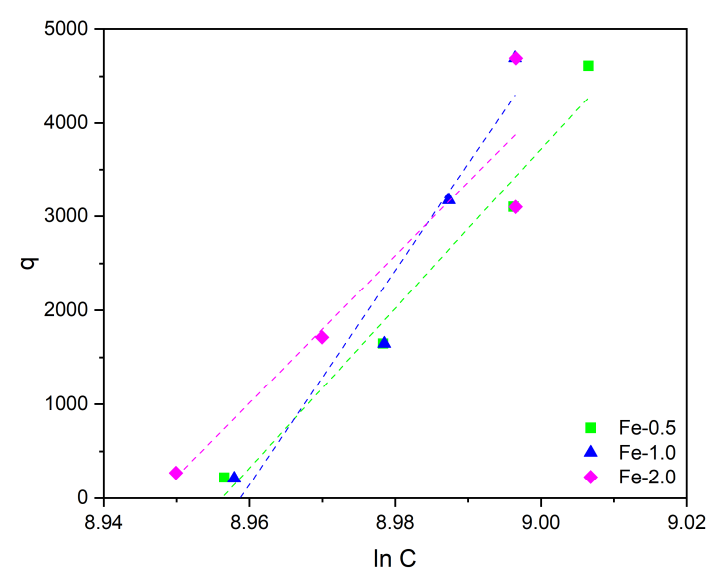


Figure 9. Temkin adsorption equilibrium of Cu onto Fe₃O₄-doped PSf membranes (pH = 7.0 ± 0.1 , membrane dosage = 1.0 g/L, contact time = 60 min, volume of feed solution = 12.5 mL)

To investigate the controlling mechanism of the adsorption kinetics, two kinetic models were used; the Lagergren's pseudo-first-order and pseudo-second-order linear models. Table 4 revealed the kinetic parameters for both models and the linear regression of the Pseudo-second-order kinetics for the adsorption of Cu(II) onto all three membranes is shown in Figure 10, respectively. From the table, it can be seen that the correlation coefficient of the linear regression (R²) for

the pseudo-second-order model was higher for all membranes (0.98-1), suggesting that the adsorption kinetics of Cu ions onto these PSf membranes obeyed the Pseudo-Second order model. In this kinetic model, the adsorption of Cu ions onto the Fe₃O₄-doped PSf membranes adopts the chemisorption process and this chemical reaction is considered the rate-limiting step. It also depends on the concentration of the Cu ions and the NPs.

Table 4. Kinetic parameters for Cu adsorption onto the Fe₃O₄-doped PSf membranes

Membrane	Parameter	Fe-0.5	Fe-1.0	Fe-2.0
Pseudo 1st order	K_1	0.0320	0.0442	0.0574
	$q_{\rm e}$	9.2452	6.6866	2.8115
	\mathbb{R}^2	0.2980	0.7361	0.9912
Pseudo 2 nd order	K_2	0.0013	0.0025	0.0274
	$q_{\rm e}$	666.6670	666.6670	270.27
	\mathbb{R}^2	0.9812	0.9991	1

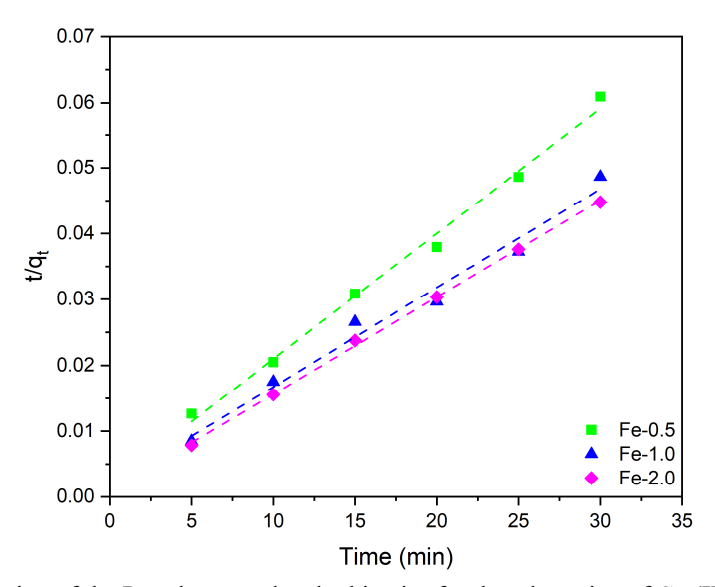


Figure 10. Linear regression of the Pseudo-second-order kinetics for the adsorption of Cu (II) onto Fe₃O₄-doped PSf membranes with various Fe₃O₄ NPs concentrations (pH = 7.0 ± 0.1 , membrane dosage = 1.0 g/L, contact time = 60 min, volume of feed solution = 12.5 mL)

The adsorption of Cu ions onto Fe₃O₄-doped PSf membranes is believed to follow four general steps; (1) bulk diffusion of Cu ions into pores of PSf membrane; (2) sorption of Cu ions onto Fe₃O₄ NPs inside the pores; (3) chemical interaction between Cu ions and Fe₃O₄ NPs through electrostatic interaction; and (4) Adsorption equilibrium reached. Figure 11 illustrates the possible

electrostatic interaction between the Cu ions and the NPs. The adsorption of Cu ions onto these Fe₃O₄ NPs that were incorporated into the PSf membrane was facilitated by the electrostatic interaction between the positive charges of Cu ions and negative charges on the Fe₃O₄ nanoparticle surface [30].

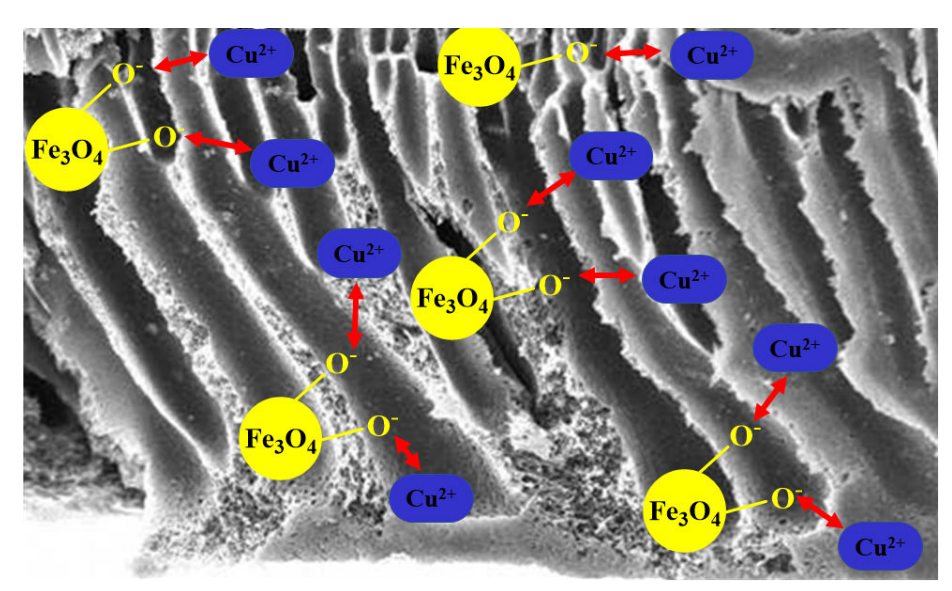


Figure 11. Schematic illustration of the possible mechanism for Cu adsorption on Fe₃O₄-doped PSf membrane

Conclusion

This work reported the synthesis of Fe₃O₄-doped PSf membranes for the removal of Cu(II) from wastewater, particularly from the electroplating industry. XRD analysis confirmed the successful synthesis of Fe₃O₄ NPs with crystallite sizes ranging from 15 to 42 nm. The Fe₃O₄-doped PSf membranes were successfully synthesized and the experimental results show a trifold increase in adsorption capability towards Cu, from 262 to 637 mg/g, proving that the Fe NPs help in improving the removal process of Cu. Membrane with 2 wt.% Fe₃O₄ showed the highest adsorption activity, credited to the easiness of Cu ions to travel to the adsorption sites, through the thicker dense layer with agglomerations. The research also revealed that the adsorption process fitted well with the Temkin isotherm and the Pseudo-second order models with coefficient correlation, R² of around ~0.98, suggesting that the adsorption process adopts the chemisorption process and is exothermic in nature. This research demonstrated the potential of incorporating Fe₃O₄ NPs into the PSf membrane matrix to improve the adsorption of Cu ions and ultimately increase Cu removal as an adsorptive membrane in membrane filtration. Further research in this direction can contribute to the development of polymeric adsorptive membranes with embedded single and alloyed transition metals, including nickel and cobalt, for effective copper and any heavy metal removal.

Acknowledgement

The authors would like to acknowledge the support from the Centre of Excellent of Biomass Utilization (CoEBU) and Centre of Excellence for Frontier Materials Research (CFMR), Universiti Malaysia Perlis (UniMAP) for assisting in sample characterizations throughout this work.

References

 Ahmed Basha, C., Bhadrinarayana, N. S., Anantharaman, N., and Meera Sheriffa Begum, K. M. (2008). Heavy metal removal from copper smelting effluent using electrochemical cylindrical flow reactor. *Journal of Hazardous Materials*, 152(1): 71-78.

- Bai, D.-K., Ying, Q.-H., Wang, N., and Lin, J.-H. (2016). Copper removal from electroplating wastewater by coprecipitation of copper-based supramolecular materials: Preparation and application study. *Journal of Chemistry*, 2016: 5281561.
- Nasir, A. M., Goh, P. S., and Ismail, A. F. (2019). Highly adsorptive polysulfone/hydrous ironnickel-manganese (PSF/HINM) nanocomposite hollow fiber membrane for synergistic arsenic removal. Separation and Purification Technology, 213, 162–175.
- 4. Liu, Y., Wang, H., Cui, Y., and Chen, N. (2023). Removal of copper ions from wastewater: A review. *International Journal of Environmental Research and Public Health*, 20(5): 3885.
- Dashtbozorg, A., Saljoughi, E., Mousavi, S. M., & Kiani, S. (2022). High-performance and robust polysulfone nanocomposite membrane containing 2D functionalized MXene nanosheets for the nanofiltration of salt and dye solutions. *Desalination*, 527: 115600.
- Qalyoubi, L., Al-Othman, A. and Al-Asheh, S. (2021). Recent progress and challenges on adsorptive membranes for the removal of pollutants from wastewater. Part I: Fundamentals and classification of membranes. Case Studies in Chemical and Environmental Engineering, 3: 100086.
- Ayaz, M., Muhammad, A., Younas, M., Khan, A. L., and Rezakazemi, M. (2019). Enhanced water flux by fabrication of polysulfone/alumina nanocomposite membrane for copper(II) removal. *Macromolecular Research*, 27(6): 565-571.
- 8. Hamid, S. A., Azha, S. F., Sellaoui, L., Bonilla-Petriciolet, A., and Ismail, S. (2020). Adsorption of copper (II) cation on polysulfone/zeolite blend sheet membrane: Synthesis, characterization, experiments and adsorption modelling. *Colloids and Surfaces A: Physicochemical and Engineering Aspects*, 601: 124980.
- Abdullah, N., Gohari, R. J., Yusof, N., Ismail, A. F., Juhana, J., Lau, W. J., and Matsuura, T. (2016). Polysulfone/hydrous ferric oxide ultrafiltration mixed matrix membrane: Preparation, characterization and its adsorptive removal of lead

- (II) from aqueous solution. *Chemical Engineering Journal*, 289: 28-37.
- Zainol Abidin, M. N., Goh, P. S., Ismail, A. F., Said, N., Othman, M. H. D., Hasbullah, H., Abdullah, M. S., Ng, B. C., Sheikh Abdul Kadir, S. H., and Kamal, F. (2019). Polysulfone/iron oxide nanoparticles ultrafltration membrane for adsorptive removal of phosphate from aqueous solution. *Journal of Membrane Science and Research*, 5(1): 20-24.
- 11. Said, N., Mansur, S., Zainol Abidin, M. N., and Ismail, A. F. (2023). Fabrication and characterization of polysulfone/iron oxide nanoparticle mixed matrix hollow fiber membranes for hemodialysis: Effect of dope extrusion rate and air gap. *Journal of Membrane Science and Research*, 9(1): 1972553.
- Rosli, A., Ahmad, A. L., and Low, S. C. (2019). Anti-wetting polyvinylidene fluoride membrane incorporated with hydrophobic polyethylenefunctionalized-silica to improve CO₂ removal in membrane gas absorption. Separation and Purification Technology, 221: 275-285.
- Wan Ramli, W. K., Liang, L. G., Othman, S., Yusri, N. A. M., and Che Lah, N. F. (2022). Phase separation behaviour modification using cosolvents on PVDF membranes for water filtration. AIP Conference Proceedings, 2541(1): 040012.
- 14. Jannah, N. R., and Onggo, D. (2019). Synthesis of Fe₃O₄ nanoparticles for colour removal of printing ink solution. *Journal of Physics: Conference Series*, 1245(1): 12040.
- 15. Mansur, S., Othman, M. H. D., Abidin, M. N. Z., Ismail, A. F., Abdul Kadir, S. H. S., Goh, P. S., Hasbullah, H., Ng, B. C., Abdullah, M. S., and Mustafar, R. (2021). Enhanced adsorption and biocompatibility of polysulfone hollow fibre membrane via the addition of silica/alphamangostin hybrid nanoparticle for uremic toxins removal. *Journal of Environmental Chemical Engineering*, 9(5): 106141.
- Dawn, R., Zzaman, M., Faizal, F., Kiran, C., Kumari, A., Shahid, R., Panatarani, C., Joni, I. M., Verma, V. K., Sahoo, S. K., Amemiya, K., and Singh, V. R. (2022). Origin of magnetization in silica-coated Fe₃O₄ nanoparticles revealed by soft

- X-ray magnetic circular dichroism. *Brazilian Journal of Physics*, 52: 99.
- 17. Upadhyay, S., Parekh, K., and Pandey, B. (2016). Influence of crystallite size on the magnetic properties of Fe₃O₄ nanoparticles. *Journal of Alloys and Compounds*, 678: 478-485.
- Singh, K., Devi, S., Bajaj, H. C., Ingole, P., Choudhari, J., and Bhrambhatt, H. (2014). Optical resolution of racemic mixtures of amino acids through nanofiltration membrane process. Separation Science and Technology, 49(17): 2630-2641.
- Mansur, S., Othman, M. H. D., Abidin, M. N. Z., Ismail, A. F., Abdul Kadir, S. H. S., Goh, P. S., Hasbullah, H., Ng, B. C., Abdullah, M. S., and Mustafar, R. (2021). Enhanced adsorption and biocompatibility of polysulfone hollow fibre membrane via the addition of silica/alphamangostin hybrid nanoparticle for uremic toxins removal. *Journal of Environmental Chemical Engineering*, 9(5): 106141.
- 20. Gohain, M. B., Pawar, R. R., Karki, S., Hazarika, A., Hazarika, S., and Ingole, P. G. (2020). Development of thin film nanocomposite membrane incorporated with mesoporous synthetic hectorite and MSH@UiO-66-NH2 nanoparticles for efficient targeted feeds separation, and antibacterial performance. *Journal of Membrane Science*, 609: 118212.
- Kumar, R., Isloor, A. M., Ismail, A. F., Rashid, S. A., and Matsuura, T. (2013). Polysulfone–chitosan blend ultrafiltration membranes: preparation, characterization, permeation and antifouling properties. *RSC Advances*, 3(21): 7855-7861.
- 22. Muntha, S. T., Ajmal, M., Naeem, H., Kausar, A., Zia, M. A., and Siddiq, M. (2019). Synthesis, properties, and applications of polysulfone/polyimide nanocomposite membrane reinforced with silica nanoparticles. *Polymer Composites*, 40(5): 1897-1910.
- 23. Rozi, S. K. M., Berhanundin, K. M., Ishak, A. R., Mohd, F. L., Rasdi, N. C. D., Rahim, N. Y., Aziz, M. Y., Shafie, F. A., and Abdullah, A. M. (2023). Novel magnetic eggshell membrane functionalized with waste palm fatty acid for selective adsorption

- of oil from aqueous solution. *Malaysian Journal of Analytical Sciences*, 27(1): 74-86.
- 24. Mansur, S., Othman, M. H., Ismail, A., Zainol Abidin, M. N., Said, N., Goh, P., Hasbullah, H., Sheikh Abdul Kadir, S. H., and Kamal, F. (2018). Study on the effect of spinning conditions on the performance of PSf/PVP ultrafiltration hollow fiber membrane. *Malaysian Journal of Fundamental and Applied Sciences*, 14: 343-347.
- 25. Kim, J. H., Kim, Y., Kim, C. K., Lee, J. W., and Seo, S. B. (2003). Miscibility of polysulfone blends with poly(1-vinylpyrrolidone-co-styrene) copoly mers and their interaction energies. *Journal of Polymer Science Part B: Polymer Physics*, 41(12): 1401-1411.
- 26. Said, N., Abidin, M. N. Z., Hasbullah, H., Ismail, A. F., Goh, P. S., Othman, M. H. D., Abdullah, M. S., Ng, B. C., Kadir, S. H. S. A., and Kamal, F. (2019). Iron oxide nanoparticles improved biocompatibility and removal of middle molecule uremic toxin of polysulfone hollow fiber membranes. *Journal of Applied Polymer Science*, 136(48): 48234.
- 27. Makhetha, T. A., and Moutloali, R. M. (2018). Antifouling properties of Cu(tpa)@GO/PES composite membranes and selective dye rejection. *Journal of Membrane Science*, 554: 195-210.
- 28. Said, N., Hasbullah, H., Ismail, A. F., Othman, M. H. D., Goh, P. S., Zainol Abidin, M. N., Sheikh Abdul Kadir, S. H., Kamal, F., Abdullah, M. S., and Ng, B. C. (2017). Enhanced hydrophilic polysulfone hollow fiber membranes with addition of iron oxide nanoparticles. *Polymer International*, 66(11): 1424-1429.
- Salar-García, M. J., Walter, X. A., Gurauskis, J., de Ramón Fernández, A., and Ieropoulos, I. (2021). Effect of iron oxide content and microstructural porosity on the performance of ceramic membranes as microbial fuel cell separators. *Electrochimica Acta*, 367: 137385.
- Mondal, M., Dutta, M., and De, S. (2017). A novel ultrafiltration grade nickel iron oxide doped hollow fiber mixed matrix membrane: Spinning, characterization and application in heavy metal removal. Separation and Purification Technology, 188: 155-166.

- Chan, K. H., Wong, E. T., Idris, A., and Yusof, N. M. (2015). Modification of PES membrane by PEG-coated cobalt doped iron oxide for improved Cu(II) removal. *Journal of Industrial and Engineering Chemistry*, 27: 283-290.
- 32. Daraei, P., Madaeni, S. S., Ghaemi, N., Salehi, E., Khadivi, M. A., Moradian, R., and Astinchap, B. (2012). Novel polyethersulfone nanocomposite membrane prepared by PANI/Fe₃O₄ nanoparticles with enhanced performance for Cu(II) removal from water. *Journal of Membrane Science*, 415: 250-259.
- Mandal, S., Calderon, J., Marpu, S. B., Omary, M. A., and Shi, S. Q. (2021). Mesoporous activated carbon as a green adsorbent for the removal of heavy metals and Congo red: Characterization, adsorption kinetics, and isotherm studies. *Journal of Contaminant Hydrology*, 243: 103869.
- 34. Fita, G., Djakba, R., Mouhamadou, S., Duc, M., Rao, S., Popoola, L. T., Harouna, M., and Benoit, L. B. (2023). Adsorptive efficiency of hull-based activated carbon toward copper ions (Cu²⁺) removal from aqueous solution: Kinetics, modelling and statistical analysis. *Diamond and Related Materials*, 139: 110421.
- Subhransu Sahoo Uma, S. B. and Sharma, Y. C. (2014). Application of natural clay as a potential adsorbent for the removal of a toxic dye from aqueous solutions. *Desalination and Water Treatment*, 52(34–36): 6703-6711.
- Elzain, A. A., El-Aassar, M. R., Hashem, F. S., Mohamed, F. M., and Ali, A. S. M. (2019). Removal of methylene dye using composites of poly (styrene-co-acrylonitrile) nanofibers impregnated with adsorbent materials. *Journal of Molecular Liquids*, 291: 111335.
- 37. Zand, A. D., and Abyaneh, M. R. (2020). Adsorption of Lead, manganese, and copper onto biochar in landfill leachate: implication of non-linear regression analysis. *Sustainable Environment Research*, 30(1): 18.
- 38. Boparai, H. K., Joseph, M., and O'Carroll, D. M. (2011). Kinetics and thermodynamics of cadmium ion removal by adsorption onto nano zerovalent iron particles. *Journal of Hazardous Materials*, 186(1): 458-465.

- Nandiyanto, A. B. D., Girsang, G. C. S., Maryanti, R., Ragadhita, R., Anggraeni, S., Fauzi, F., Sakinah, P., Astuti, A. P., Usdiyana, D., Fiandini, M., Dewi, M. W., and Al-Obaidi, A. S. M. (2020). Isotherm adsorption characteristics of carbon microparticles prepared from pineapple peel waste. *Communications in Science and Technology*, 5(1): 31-39.
- 40. Karim, K. H. (2020). Copper adsorption behavior in some calcareous soils using Langmuir, Freundlich,
- Temkin, and Dubinin-Radushkevich models. Journal of Soil Sciences and Agricultural Engineering, 11(1): 27-34.
- 41. van den Berg, T. and Ulbricht, M. (2020). Polymer nanocomposite ultrafiltration membranes: The influence of polymeric additive, dispersion quality and particle modification on the integration of zinc oxide nanoparticles into polyvinylidene difluoride membranes. *Membranes*, 10(9): 197.